

Effects of load height application and pre-buckling deflections on lateral buckling of thin-walled beams

F. Mohri^{1,2†} and M. Potier-Ferry^{2‡}

¹UT Nancy-Brabois, Département Génie Civil, Université Henri Poincaré, Nancy 1,
54601 Villers les Nancy, France

²LPMM, UMR CNRS 7554, ISGMP, Université Paul Verlaine-Metz, Ile du Saulcy,
57045 Metz, France

(Received November 16, 2005, Accepted May 23, 2006)

Abstract. Based on a non-linear model taking into account flexural-torsional couplings, analytical solutions are derived for lateral buckling of simply supported I beams under some representative load cases. A closed form is established for lateral buckling moments. It accounts for bending distribution, load height application and pre-buckling deflections. Coefficients C_1 and C_2 affected to these parameters are then derived. Regard to well known linear stability solutions, these coefficients are not constant but depend on another coefficient k_1 that represents the pre-buckling deflection effects. In numerical simulations, shell elements are used in mesh process. The buckling loads are achieved from solutions of eigenvalue problem and by bifurcations observed on non linear equilibrium paths. It is proved that both the buckling loads derived from linear stability and eigenvalue problem lead to poor results, especially for I sections with large flanges for which the behaviour is predominated by pre-buckling deflection and the coefficient k_1 is large. The proposed solutions are in good agreement with numerical bifurcations observed on non linear equilibrium paths.

Keywords: buckling; finite element; eigenvalue; linear stability; non linear stability; open section; pre-buckling; thin-walled beam.

1. Introduction

Steel and composite structures made in thin-walled are very sensitive to stabilities. Usually, elastic buckling loads of a structure can be computed in two steps. The first, based on first order assumption leads to a estimation of buckling loads using classical linear stability models or from solution of eigenvalue problem. Nevertheless, the obtained results are not sufficient and it is necessary to obtain buckling loads more accurately. For this aim, the non linear behaviour of the structure must be undertaken in a second step with consideration of geometric imperfections. This leads to the equilibrium path until the post-buckling range. Then, the real buckling loads are captured.

Most of stability analyses of thin-walled beams ignore the pre-buckling effects (Barsoum 1970, Bazant 1973, Laudiero 1988). Nevertheless, it is proved that the pre-buckling deformations have a predominant influence on beam lateral buckling. It results from non-linear couplings between the two bending

†Assistant Professor, Corresponding author, E-mail: Foudil.Mohri@iutnb.uhp-nancy.fr

‡Professor

curvatures and is then function on bending stiffness ratio. Yet, the effect of pre-buckling deflections on beam lateral buckling strength had been investigated essentially in the case of pure bending moments by Vacharajittiphan (1974) and more recently by Achour (2000). This solution is frequently used as a benchmark reference for validation of finite element models (Ronagh 2000, Pi 2001). Another solution has been derived by Mohri (2002) in the case of a beam under distributed loads including the load height parameter and pre-buckling effects.

In this paper, a model is developed in large torsion context taking into account for flexural-torsional couplings. Load eccentricities, pre-buckling deflections and non linear warping are considered. An improved compact analytical expression is investigated and extended to lateral buckling resistance of beams under some representative load cases including uniform and concentrated loads. Bending distribution, pre-buckling deformations and load height effects are included in the solution. These proposed solutions are compared to the classical ones commonly used in linear stability and design and validated by recourse to a non-linear shell finite element package.

2. Overview of a non-linear model for thin-walled elements

2.1. Equilibrium equations

In a previous work, Vlasov’s model has been extended to large displacements and non-linear stability analyses (Mohri 2001). A straight thin-walled element with an open section is pictured in Fig. 1 and a direct rectangular co-ordinate system has been chosen. x denotes the initial longitudinal axis and y and z are the principal bending axes. The origin of these axes is located at the centre G . The shear centre with co-ordinates (y_c, z_c) in Gyz is denoted C . Consider M , a point on the section contour with its co-ordinates (y, z, ω) where ω is the sectorial co-ordinate used in Vlasov’s model. Based on the usual assumptions of the theory of thin-walled elements, displacement components of the point M can be derived from those of the shear centre:

$$u_M = u - y(v' \cos \theta_x + w' \sin \theta_x) - z(w' \cos \theta_x - v' \sin \theta_x) - \omega \theta_x' \tag{1}$$

$$v_M = v - (z - z_c) \sin \theta_x - (y - y_c)(1 - \cos \theta_x) \tag{2}$$

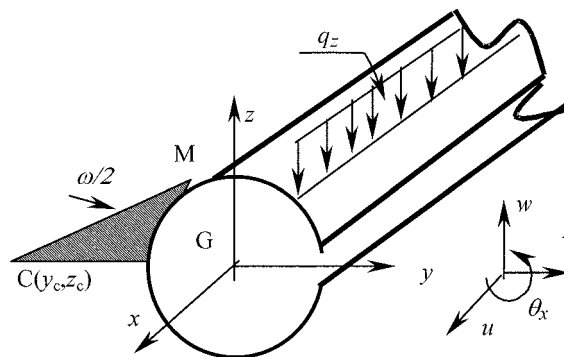


Fig. 1 An open section beam

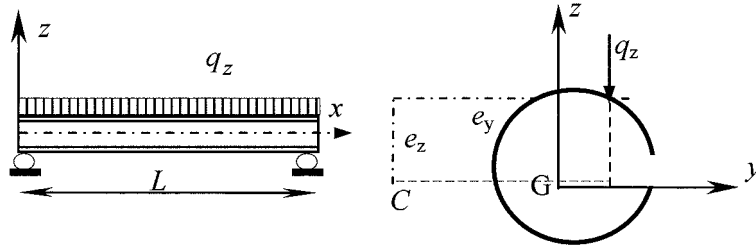


Fig. 2 Beam element under eccentric distributed load

$$w_M = w + (y - y_c) \sin \theta_x - (z - z_c)(1 - \cos \theta_x) \quad (3)$$

In these formulations, u is the axial displacement of centroid G , v and w are displacement components of shear centre C in y and z directions. θ_x is the torsion angle of the shear center. The x -derivative is denoted $(\cdot)'$. The expressions of displacement components of M given by (1-3) are then non-linear and depend on the approximation done for circular functions $\cos \theta_x$ and $\sin \theta_x$. Let us recall that linear stability models are derived from (1-3) by using the approximation $\cos \theta_x = 1$ and $\sin \theta_x = \theta_x$ and by disregarding the resulting non-linear terms (Timoshenko 1961, Trahair 1993, Barsoum 1970, Bazant 1973). Equilibrium equations are formulated from the stationary conditions:

$$\delta \left(\int_V \sigma_{ij} \varepsilon_{ij} dv - W \right) = 0 \quad (4)$$

where δ denotes virtual variation. σ_{ij} is the Piola-Kirchhoff stress tensor. ε_{ij} represents the Green strain tensor which incorporates large displacements. W is the external load work which is reduced for simplicity in the present work to distributed vertical loads q_z with eccentricities e_y and e_z measured from shear centre point (Fig. 2).

In non linear stability models, differential equilibrium equations are computed under consideration of non-linear relationships between bending moments and curvatures and with non linear approximations for circular functions. In the present work, they are the following:

$$\cos \theta_x = 1 - \frac{\theta_x^2}{2}, \quad \sin \theta_x = \theta_x - \frac{\theta_x^3}{6} \quad (5a,b)$$

After some calculations, in the case of elastic behaviour, the coupled flexural-torsional equilibrium equations are derived and arranged as:

$$EI_z \left(v^{(4)} + 3v'v''v''' + v''^3 + \frac{v^{(4)}v'^2}{2} \right) + (EI_z - EI_y)(w^{(4)}\theta_x + 2w''' \theta_x' + w'' \theta_x'' - v^{(4)}\theta_x^2 - 4v''' \theta_x \theta_x' - 2v'' \theta_x \theta_x'' - 2v'' \theta_x'^2) = 0 \quad (6)$$

$$EI_y \left(w^{(4)} + 3w'w''w''' + w''^3 + \frac{w^{(4)}w'^2}{2} \right) + (EI_z - EI_y)(v^{(4)}\theta_x + 2v''' \theta_x' + v'' \theta_x'' + w^{(4)}\theta_x^2 + 4w''' \theta_x \theta_x' + 2w'' \theta_x \theta_x'' + 2w'' \theta_x'^2) = q_z \quad (7)$$

$$EI_{\omega}\theta_x^{(4)} - GJ\theta_x'' - \frac{3}{2}EI_t\theta_x'^2\theta_x'' + (EI_z - EI_y)(v''w'' - v''^2\theta_x + w''^2\theta_x) = q_z(e_y - e_z\theta_x) \quad (8)$$

In these differential equations, $(\cdot)''(\cdot)'''$ and $(\cdot)^{(4)}$ denote x -derivative of order 2, 3 and 4. E and G are axial and shear constants. I_y and I_z are the second moments of area about the principal axes y and z . J and I_{ω} are respectively the St-Venant torsion and the warping constants. I_t denotes the fourth moment of area about the shear centre. A numerical procedure for the computation of these geometric characteristics is described in Mohri (2001).

In the case of simply supported conditions in both bending and torsion with free warping, a realistic function for the displacement v , w and θ_x in the first mode is:

$$v = v_0\sin\left(\pi\frac{x}{L}\right), \quad w = w_0\sin\left(\pi\frac{x}{L}\right), \quad \theta_x = \theta_0\sin\left(\pi\frac{x}{L}\right) \quad (9a-c)$$

v_0 , w_0 and θ_0 are the associated displacement amplitudes. In order to solve the non-linear differential system (6-8), Galerkin's approximation method is first applied. After integration and some calculations, the three coupled equilibrium equations written in compact form are:

$$P_z\left(v_0 + \frac{\pi^2}{8L^2}v_0^3\right) + (P_z - P_y)\left(\frac{8}{3\pi}w_0\theta_0 - \frac{3}{4}v_0\theta_0^2\right) = 0 \quad (10)$$

$$P_y\left(w_0 + \frac{\pi^2}{8L^2}w_0^3\right) + (P_z - P_y)\left(\frac{8}{3\pi}v_0\theta_0 + \frac{3}{4}w_0\theta_0^2\right) - \frac{32}{\pi^3}M_0 = 0 \quad (11)$$

$$I_0P_{\theta}\theta_0 + \frac{3\pi^2EI_t}{8L^2}\theta_0^3 + (P_z - P_y)\left(\frac{8}{3\pi}v_0w_0 - \frac{3}{4}\theta_0v_0^2 + \frac{3}{4}\theta_0w_0^2\right) + \left(\frac{8}{\pi^2}e_z\theta_0 - \frac{32}{\pi^3}e_y\right)M_0 = 0 \quad (12)$$

In these algebraic equations, M_0 is the maximal bending moment of the beam. P_y and P_z , are the Euler's buckling loads. P_{θ} is the pure torsion buckling load and I_0 is the polar moment of area. They are given by the following relationships:

$$P_y = \frac{\pi^2EI_y}{L^2} \quad (13)$$

$$P_z = \frac{\pi^2EI_z}{L^2} \quad (14)$$

$$P_{\theta} = \frac{1}{I_0}\left(\frac{\pi^2EI_{\omega}}{L^2} + GJ\right) \quad (15)$$

$$M_0 = \frac{q_zL^2}{8} \quad (16)$$

At this stage, one can remark that equilibrium equations obtained are all non linear and highly coupled. Again, in the torsion equilibrium Eq. (12) a cubic term in θ_0 is present and is called the shortening or non-linear warping term.

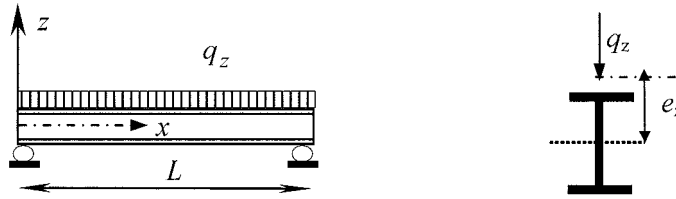


Fig. 3 A beam under distributed load and definition of load height parameter e_z

2.2. Computation of lateral buckling loads

When one deals with non-linear equations, one can remind that the solution is not unique and becomes more complex in presence of singular points. First, when this is possible, analyst can be helped when the singular points can be estimated. In beam lateral buckling, bifurcation happens when the load q_z or the equivalent bending moment M_0 is applied to the beam without any eccentricity e_y (Fig. 3). In this context, the beam moves vertically, what corresponds to the pre-buckling state, also called ‘the fundamental state’. When the buckling load is reached, the behaviour of the beam is suddenly flexural-torsional. Displacements components in the fundamental state are in the form $\{v_0, w_0, \theta_0\}^t = \{0, w_0, 0\}$. The buckling loads are computed from singular points of the tangential matrix of the non-linear system (10-12). This leads to a quadratic equation combining bending moment M_0 and deflection w_0 as formulated in Mohri (2002).

$$P_z \left[\frac{\pi^2 EI_\omega}{L^2} + GJ + \frac{3}{4}(P_z - P_y)w_0^2 + \frac{8}{\pi^2}M_0e_z \right] - \frac{64}{9\pi^2}(P_z - P_y)^2 w_0^2 = 0 \quad (17)$$

In fundamental state, beam deflection w_0 can be easily related to the applied moment M_0 using first order assumptions in (11). One gets:

$$w_0 = \frac{32M_0}{\pi^3 P_y} \quad (18)$$

By using the relationships of P_y and M_0 given in (13,16), this relationship is easily reduced to the well known formula used in the literature $\left(w_0 = \frac{5}{384} \frac{q_z L^4}{EI_y} \right)$. Incorporation of (18) in (17) yields to a quadratic equation that depends only on M_0 . The final expression of the buckling moment M_0 , denoted by $M_{0,b}(nl)$, is:

$$M_{0,b}(nl) = C_1 \frac{\pi^2 EI_z}{L^2} \left[(C_2 e_z) \pm \sqrt{(C_2 e_z)^2 + \frac{I_\omega}{I_z} \left(1 + \frac{GJL^2}{\pi^2 EI_\omega} \right)} \right] \quad (19)$$

where
$$C_1 = \frac{1.14}{\sqrt{k_1}} \quad C_2 = \frac{0.46}{\sqrt{k_1}} \quad \text{and} \quad k_1 = 1 - \frac{I_z}{I_y} \quad (20a-c)$$

According to models developed from linear stability as in Trahair’s book (Trahair 1993) or solutions adopted in (Eurocode 3 1992), a similar expression is used with constant values for the coefficients C_1

and C_2 , respectively equal to $C_1=1.13$, $C_2=0.46$. In the present model which includes the effects of the pre-buckling deflections, these coefficients are not constant but depend on the section shapes and represented by the coefficient k_1 that is function on the geometric ratio I_z/I_y . Referred to (20), for a section with a highly bending resistance about the y -axis ($I_y \gg I_z$), the coefficient k_1 is close to 1.0 and the coefficients C_1 and C_2 are reduced to values usually found in linear stability. But, when a section beam has an equivalent bending resistance about the two principal axes y and z ($I_y \approx I_z$), the coefficients C_1 and C_2 are very different from the constant values found within linear stability. Obviously, for such section shapes, the difference between the linear and non-linear stability should be very important. Again, when the inertial moment are close ($I_y = I_z$), the coefficient k_1 vanishes. The beam resistance to lateral buckling becomes infinitely large.

Also, the present model can be employed in lateral buckling of beams under concentrated loads. In such situations, Dirac's function is used and the same procedure can be followed as discussed in Mohri (2003). As an example, in the case of a beam under two concentrated loads Q_z applied at $L/4$, the relationship (17) is fulfilled but the relationships between load (Q_z, M_0) and (M_0, w_0) are the following:

$$M_0 = Q_z \frac{L}{4} \quad w_0 = \frac{11\pi^2 M_0}{96 P_y} \quad (21a,b)$$

The expression of the buckling moment is similar to (19) but the coefficients C_1 and C_2 in (20a-b) are exchanged respectively into:

$$C_1 = \frac{1.042}{\sqrt{k_1}} \quad C_2 = \frac{0.422}{\sqrt{k_1}} \quad (22a,b)$$

In the case of a beam under two concentrated loads Q_z applied at $L/3$, the bending moment and the deflection are:

$$M_0 = Q_z \frac{L}{3} \quad w_0 = \frac{13\pi^2 M_0}{72 P_y} \quad (23a,b)$$

The buckling moment Eq. (19) is obtained with coefficients C_1 and C_2 given by:

$$C_1 = \frac{1.121}{\sqrt{k_1}} \quad C_2 = \frac{0.511}{\sqrt{k_1}} \quad (24a,b)$$

Remind that from linear stability, one yields for these load cases constant coefficients independent of the ratio I_z/I_y . They are respectively equal to $C_1=1.05$, $C_2=0.43$ for loads applied at $L/4$ and $C_1=1.10$, $C_2=0.50$ for loads applied at $L/3$.

Also, when the beam is loaded only by a concentrated load applied at mid-span, one uses in (19) the following values for C_1 and C_2 and for M_0 :

$$C_1 = \frac{1.36}{\sqrt{k_1}} \quad C_2 = \frac{0.55}{\sqrt{k_1}} \quad M_0 = Q_z \frac{L}{4} \quad (25a-c)$$

The importance of the pre-buckling deflections on the lateral buckling of beams has been outlined since 1974 by Vacharajittiphan (1974) in the case of a bisymmetric I-beam under end uniform bending. More recently, Achour (2000) obtained the same analytical expression as in Vacharajittiphan (1974).

Referred to the nomenclature adopted in the present work, the buckling moment formulated in Vacharajittiphan and Achour works can be written as:

$$M_{0,b}(nl) = \frac{M_{0,b}(lin)}{\sqrt{k_1}\sqrt{k_2}} \quad (26a)$$

where $M_{0,b}(lin)$ is the classical buckling moment of a beam derived from linear stability in pure bending:

$$M_{0,b}(lin) = \sqrt{\frac{\pi^2 EI_z}{L^2} \left(GJ + \frac{\pi^2 EI_\omega}{L^2} \right)} \quad \text{or} \quad M_{0,b}(lin) = \frac{\pi^2 EI_z}{L^2} \sqrt{\frac{I_\omega}{I_z} \left(1 + \frac{GJL^2}{\pi^2 EI_\omega} \right)} \quad (26b)$$

k_1 is the same as (20c) and k_2 is an additional geometric constant given by:

$$k_2 = 1 - \frac{GJ}{EI_y} \left(1 + \frac{\pi^2 EI_\omega}{GJL^2} \right) \quad (26c)$$

After some manipulations, one can easily check that the relationship (26a) is consistent with (19). For this load case, the C_2 coefficient is insignificant for axial moments and coefficient C_1 is written as:

$$C_1 = \frac{1.0}{\sqrt{k_1}\sqrt{k_2}} \quad (26d)$$

Hereafter, we will investigate the importance of the additional coefficient k_2 on beam lateral buckling and it will be proved that the value of k_2 in (26c) is often close to 1.0 for most of usual standard cross sections. Its contribution can reasonably be omitted.

So, the compact relationship (19) with the coefficients C_1 and C_2 depending on bending distributions, load height parameter and including the pre-buckling deflections constitutes an improved and original formulation that predict accurately the beam lateral buckling under some representative load cases and for any bi-symmetric I section shape and can be applied to other section shapes such as channel sections under some requirements for load applications.

At this stage, it is important to compare the present solutions to those presented in Roberts and Burt (1985). Following the nomenclature adopted in the present work, the buckling loads of a bisymmetric I section under uniform moment, a concentrated central load Q_z or distributed load q_z including load height parameter are given by:

For uniform bending:
$$M_{0,b} = \lambda_1 \frac{\sqrt{EI_z GJ}}{L} \quad (27a)$$

For concentrated load:
$$Q_z = \lambda_2 \frac{\sqrt{EI_z GJ}}{L^2} \quad (27b)$$

For distributed load
$$q_z = \lambda_3 \frac{\sqrt{EI_z GJ}}{L^3} \quad (27c)$$

Coefficients λ_1, λ_2 and λ_3 are derived in terms of Wagner’s term, torsion constants, load height level and pre-buckling deflection effects. Their expressions are shown in Roberts and Burt (1985). Solutions (27) have been modified in order to get the compact closed form solution (19). It can be proved that (27a) is straightforward. Relationships (27b) is first changed to equivalent buckling moment according to (25c). After some manipulations on the obtained buckling moment relationship, one gets for C_1 and C_2 the following values:

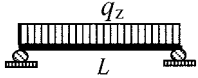
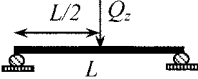
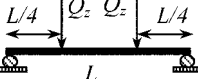
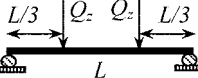
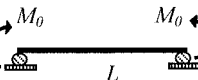
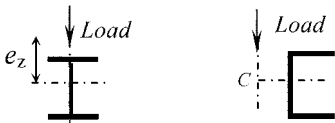
$$C_1 = \frac{\sqrt{294}}{4\pi\sqrt{1 - \frac{I_z}{I_y}}} \quad C_2 = \frac{29.85}{\pi\sqrt{294}\sqrt{1 - \frac{I_z}{I_y}}} \quad (28a,b)$$

These coefficients are close to (25a,b). Again Eq. (27c) is first changed to equivalent buckling moment according to (16) and the obtained expression is modified in accordance to (19). For this load case, one obtains for coefficients C_1 and C_2 :

$$C_1 = \frac{\sqrt{810}}{8\pi\sqrt{1 - \frac{I_z}{I_y}}} \quad C_2 = \frac{41.1}{\pi\sqrt{810}\sqrt{1 - \frac{I_z}{I_y}}} \quad (29a,b)$$

One can easily check that these values agree well with (20a,b).

Table 1 Improved C_i coefficients for different load cases

Load case	M_0	C_1	C_2
	$q_z \frac{L^2}{8}$	$\frac{1.13}{\sqrt{k_1}}^*$	$\frac{0.46}{\sqrt{k_1}}^*$
	$Q_z \frac{L}{4}$	$\frac{1.36}{\sqrt{k_1}}^*$	$\frac{0.55}{\sqrt{k_1}}^*$
	$Q_z \frac{L}{4}$	$\frac{1.05}{\sqrt{k_1}}^*$	$\frac{0.43}{\sqrt{k_1}}^*$
	$Q_z \frac{L}{3}$	$\frac{1.10}{\sqrt{k_1}}^*$	$\frac{0.50}{\sqrt{k_1}}^*$
	M_0	$\frac{1.0}{\sqrt{k_1}}^*$	
			(*): $k_1 = 1 - \frac{I_z}{I_y}$

2.3. Summary of the proposed solutions

Before the validation approach, the authors believe that it is important to summarise the principal ideas discussed previously. An improved analytical solution is proposed for checking the lateral buckling strength of bi-symmetric I and Channel sections. It includes the load bending distribution, load height parameter for distributed and concentrated loads and pre-buckling deflections. The analytical solution is reminded below:

$$M_{0,b}(nl) = C_1 \frac{\pi^2 EI_z}{L^2} \left[(C_2 e_z) \pm \sqrt{(C_2 e_z)^2 + \frac{I_\omega}{I_z} \left(1 + \frac{GJL^2}{\pi^2 EI_\omega} \right)} \right] \quad (30)$$

The coefficients C_1 and C_2 are given in Table 1 for some representative load cases. These coefficients are functions on the geometric ratio I_z/I_y . These analytical solutions are valid for simply supported beams in both bending and torsion. It has been admitted that the load axis is passing through shear centre. The load height parameter e_z should be indifferent, but initial torsion must vanish.

3. Illustrative examples

3.1. Finite element modelling of beam lateral buckling

In numerical approach, attention is focused on the importance of the pre-buckling deflection and on load height parameter effects on beam lateral buckling resistance. Three load cases are considered in the study: beam under uniformly distributed load, beam under concentrated load at mid-span and beam under uniform bending moments. The results are similar for the other load cases. The beam section is a standard HEA 200. For this section, the flanges width (200 mm) is approximately of the same order as the height (190 mm). The ratio I_z/I_y of order 0.38 is large. The geometric characteristics of the sections are computed according to the numerical procedure originally developed in Mohri (2001). The steel elastic constants are $E = 210$ and $G = 80.77$ GPa.

For each load case, analytical solutions resulting from classical linear stability and the proposed solutions formulated here from non-linear stability are compared to numerical simulations. In numerical results, Abaqus finite element code is customized (Hibbit, Karlsson and Sorensen Inc 2003). Each beam is modelled with thin-walled shell elements (S8R5). For the purpose, uniform mesh has been assumed for web and flanges. In engineer practices, it is frequent that stability analysis is limited to buckling loads derived only from solutions of eigenvalue problem without considering imperfections. The resulting solutions show a qualitative estimation of the real buckling loads and must be considered cautiously. To determine the real buckling load more accurately, it is necessary that eigenvalue solutions must be validated by considering the entire non-linear load-deflection response of the member, with eventually account for imperfections. Unfortunately, this last process is very difficult to obtain and time consuming. This is the reason why analytical or eigenvalue problem solutions are more popular and preferred in usual engineering design. In what follows, numerical buckling loads result from the two techniques.

When one deals with buckling analysis of thin-walled beams using shell elements, many problems should be encountered such as distortional modes and local buckling effects affecting area of concentrated loads and boundary conditions (Fig. 4a). All these phenomena are naturally ignored in

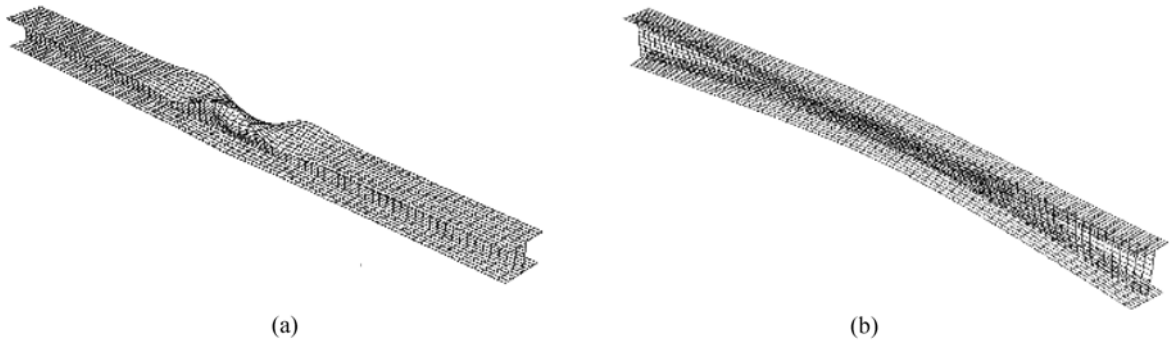


Fig. 4 (a) Undesirable local mode due to concentrated load, (b) Overall mode in beam lateral buckling

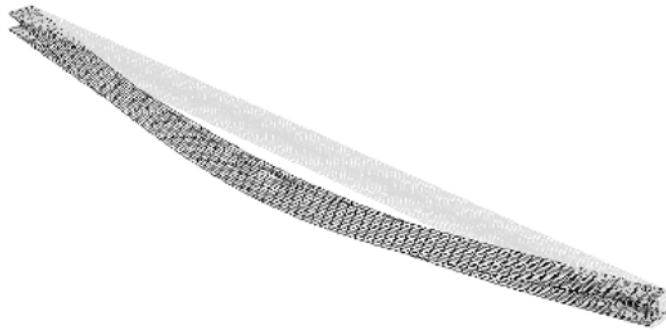


Fig. 5 Initial and flexural-torsional states of I beam in lateral post-buckling behaviour

previous analytical formulations derived from beam theory. Nevertheless, in order to reduce the effects of these undesirable modes, only slender beams are considered and attention is focused on research of overall buckling modes (Fig. 4b). It is well known that in non-linear pre-buckling ranges, the beam response is essentially flexural. The displacement is reduced to a deflection w in z direction. When the buckling load is reached, the beam behaviour becomes suddenly flexural-torsional. Additional displacements v in y direction and torsion θ_x arise in post-buckling range. Fig. 5 depicts beam deformation at the end of process in post-buckling range. In order to initiate the flexural-torsional behaviour of the beam, initial twist moment and a concentrated load in y directions are applied at mid-span. These loads lead to initial small imperfections. For each beam, the displacements v_0 and w_0 of the shear centre at the middle of the beam are followed and their variation with respect to load or relating bending moment are pictured. Due to the nature of the equilibrium equations and the presence of singular points, Riks method is adopted in the path-following.

3.2. Beam under distributed loads

The equilibrium paths (M_0, v_0) in pre-buckling and post-buckling states are plotted in Fig. 6(a), for a beam slenderness $L = 6$ m. Three load positions have been investigated, top flange, shear centre and bottom flange. One can observe that the displacements v_0 are present only in post-buckling range. The equilibrium paths (M_0, w_0) in pre-buckling and post buckling states are depicted in Fig. 6(b), for the three load heights. In pre-buckling range, the deflection w_0 is linear, agrees well with relationship (18)

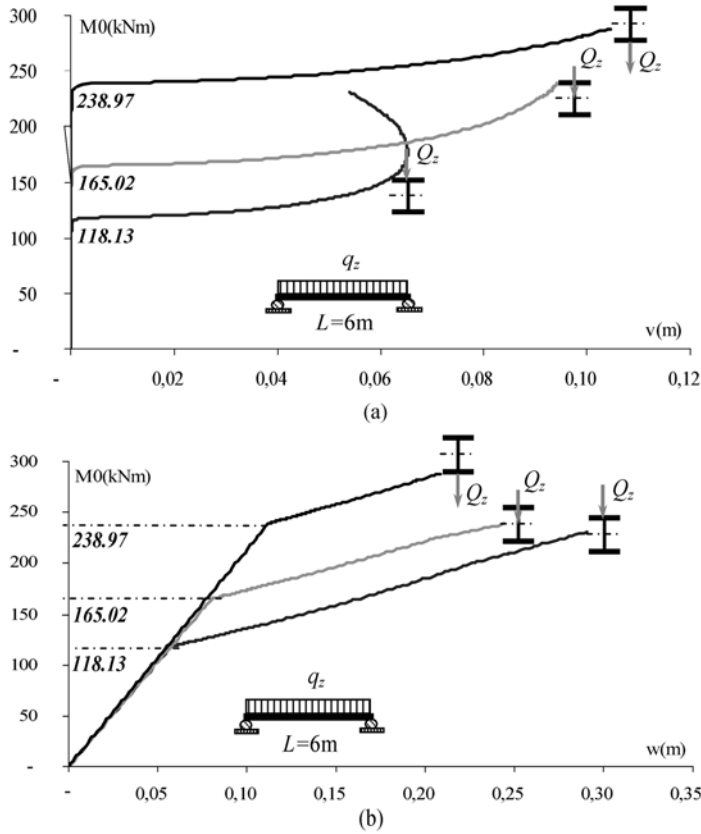


Fig. 6 (a) (M_0, v) beam response for three load positions under distributed load, (b) Beam deflections for three load positions under distributed load

and is independent from the load position. These curves have the same tendencies and present a stable post-buckling behaviour for the three load positions. This means that the beam has some reserve in post-buckling range. Bifurcation points are load height dependent. They are respectively observed at 118.13 for load on top flange, 165.02 when load is on shear centre and 238.97 kNm for load on bottom flange. Buckling moments computed according to eigenvalue problem lead to 101.61, 135.54 and 174.25 respectively for loads on top, shear and bottom flanges. Analytical buckling moments according to linear and non-linear stability models have been computed and compared to shell results. Buckling moments resulting from classical linear stability are obtained from relationship (19), but the coefficients C_1 and C_2 are kept constant respectively to $C_1 = 1.14$, $C_2 = 0.46$. The buckling moment of the beam according to non-linear stability are derived from the compact analytical solution (19) which includes the pre-buckling deflections. Here, as mentioned in relation (20a,c), the coefficients C_1 and C_2 are functions on the ratio I_z / I_y . Analytical and numerical results are summarized in Table 2 for the three load positions. Some comments are needed:

- The numerical buckling moments resulting from bifurcations relating to non-linear behaviour agrees with analytical solutions proposed from non-linear stability. The difference is less than 1%,
- eigenvalue problem solutions are close to linear stability values for the three load positions,

Table 2 Analytical linear and non-linear bifurcation moments and comparison to numerical buckling moments. Beam of slenderness 6 m under distributed load q_z , values in kNm

	Linear stability (analytic)	Shell (EVP)	Non-linear stability (analytic)	Shell (non-linear)
Top flange	101.77	101.61	119.87	118.13
Shear centre	134.47	135.54	170.09	165.02
Bottom flange	177.68	174.25	241.33	238.97

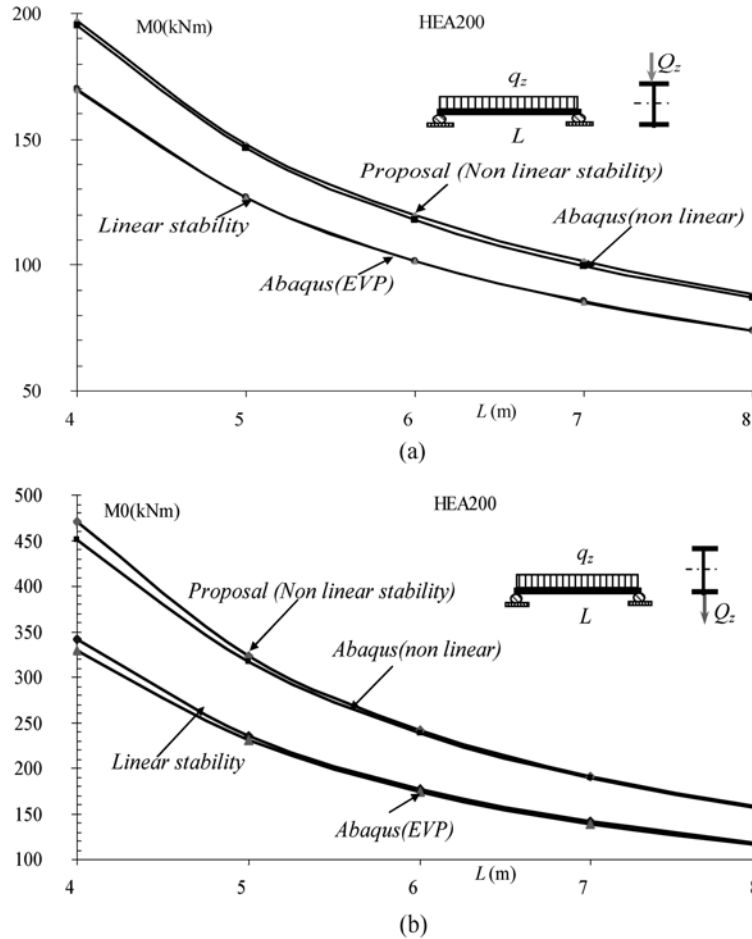


Fig. 7 (a) Analytical and numerical buckling moment variations versus L , load on top flanges, (b) Analytical and numerical buckling moment variation versus L , load on bottom flanges

- In spite of imperfections, bifurcations deduced from non-linear shell behaviour lead to higher buckling moments than those predicted by linear stability and eigenvalue problem.
- linear stability and eigenvalue problem solutions underestimate tremendously the real lateral buckling resistance of beams for which the behaviour is predominated by pre-buckling deflections such as I sections with large flanges. For this slenderness, the difference is of order 15% when load is on top flange and can reach 30% when load is applied on bottom flange.

In order to outline the importance of pre-buckling deflection on lateral buckling stability, an extensive study has been done by varying slenderness L . The elastic buckling moment variation versus L are reported in Fig. 7(a) for load on top flange and in Fig. 7(b) for load on bottom flange. Analytical results according to classical linear and proposed non-linear stability are reported and compared numerical solutions resulting from eigenvalue problem (EVP) and singular points along the non linear equilibrium paths (*non linear*). One can check that the difference of buckling moments resulting from the classical stability and eigenvalue problem with regard to buckling moments computed from non-linear stability is very impressive. They are very conservative for the two load positions and for all the practical beam slenderness L . The difference is of order 17% when load is on top flange and can reach 36% for load on bottom flange. On the other hand, the agreement between buckling moments computed from non-linear bifurcations and the proposed solutions is excellent. Effectively, for sections with large ratio I_z/I_y , the lateral buckling resistance of beams is predominated by pre-buckling deformations. The linear stability leads to poor results and cannot predict correctly the real lateral buckling resistance. For such sections, the proposed improved solutions should lead to important cost and weight savings.

3.3. Beam under a concentrated load

For this load case, the equilibrium paths curves have the same tendency as the previous load case. For this reason they are not shown. Singular points are again load height dependant. Singular points observed along the equilibrium curves are respectively produced for the three load positions at 131 kNm when load is on top flange, 195 kNm for load applied to shear centre and 297.46 kNm when load acts on bottom flange. Solutions of eigenvalue problem lead to buckling moments respectively equal to 114.74, 56.35 and 222.68.

Analytical buckling moments resulting from linear and non-linear stability models have been computed. Non-linear stability buckling moments are obtained according to relationship (19). Coefficients C_1 and C_2 related to this load case formulated in (25a,b) include pre-buckling deflection effects. They are function on the ratio I_z/I_y . For linear stability solutions, closed form Eq. (19) is used but coefficients C_1 and C_2 are kept constant respectively to $C_1 = 1.36$, $C_2 = 0.55$. Analytical and numerical results are summarized in Table 3 for the three load positions. One can remark:

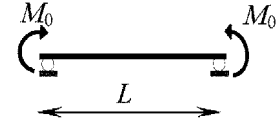
- The numerical buckling moments relating bifurcations observed equilibrium paths agrees with analytical solutions proposed from non-linear stability. The difference is less than 2%,
- linear stability values are close to solutions of eigenvalue problems for the three load positions but these solutions are lower than non-linear stability values. For this slenderness ($L = 6$ m), the difference is of order 15% when load is on top flange and can reach 30% when load is applied on bottom flange.

Table 3 Linear and non-linear bifurcation moments and comparison to numerical buckling moments, beam of slenderness 6 m under concentrated load at 3 m, values in kNm

	Linear stability (analytic)	Shell (EVP)	Non-linear stability (analytic)	Shell (non-linear)
Top flange	115.7	114.74	134.6	131.00
Shear centre	161.27	156.35	203.98	195.00
Bottom flange	224.79	222.68	309.13	297.46

Table 4 Beam under uniform bending: comparison of analytical solution for buckling moments, related to linear and non-linear stability models, values in kNm

L(m)	$M_{0,b}(lin)$	$M_{0,b}(nl, k_1)$	$M_{0,b}(nl, k_1, k_2)$
4	212.28	268.51	268.04
5	152.55	192.96	192.69
6	118.58	149.99	149.81
7	96.96	122.64	122.50
8	82.07	103.80	103.70



3.4. Beam under uniform bending

Let us now investigate the importance of the pre-buckling deflections on the lateral buckling of beams under uniform bending. Referred to relationship (26) originally investigated in (Vacharajittiphan 1974, Achour 2000), one can remark the presence of an additional coefficient k_2 , formulated in (26c). For this aim, buckling moments of the beam for some practical slenderness L are presented in Table 4. The buckling moments are computed according to linear and non-linear stability. Classical linear stability results $M_{0,b}(lin)$ are in column 2. The coefficient C_1 is kept constant ($C_1 = 1.0$). The buckling moments of the beam ($M_{0,b}(nl, k_1)$ with coefficient C_1 function only on k_1 follow in column 3. Non-linear stability results including both coefficients k_1 and k_2 are denoted $M_{0,b}(nl, k_1, k_2)$. They are arranged at the last column 4. As in the previous example, one can observe that the linear stability underestimates greatly beam lateral buckling capacity and shows poor results with reference to non-linear stability. The buckling moments $M_{0,b}(nl, k_1)$ and $M_{0,b}(nl, k_1, k_2)$ coincide. For this example, we have observed that the main value of coefficient k_2 averages 0.996. Other comparisons have been done on some standard H-sections shapes ranging from HEA100 to HEA1000 and lead to k_2 close to 1. The effect of this coefficient is not so important. Improved solutions are sufficient with only the coefficient k_1 . In engineering practice, it is then acceptable and usual to disregard the k_2 coefficient.

4. Conclusions

In this paper, non-linear stability analysis of thin-walled open section beams has been investigated. The equilibrium equations are deduced in the context of large displacements, taking into account for warping, shortening and couplings between bending and torsion. It has been established that the lateral buckling loads are highly dependent on bending distribution, on load height parameter and on pre-buckling deflections. Improved analytical solutions are provided for the lateral buckling resistance of beams with bisymmetric I or Channel sections. The coefficients C_1 and C_2 are given for some representative load cases. These coefficients are function on the geometric ratio $k_1 = 1 - I_z^2/I_y$.

Analytical solutions have been compared to finite element model using shell elements. Buckling moments have been computed from solutions of eigenvalue problem of from singular points observed along the non-linear equilibrium paths. Attention has been focused on effects of load height parameter and on geometric ratio k_1 . It has been demonstrated that linear stability and buckling eigenvalue solutions are not appropriate for sections where the behaviour is predominated with pre-buckling deflection. The proposed solutions predict well beam lateral buckling resistance independently of section shape and are close to singular points of non linear equilibrium curves.

References

- Achour, B. and Roberts, T. M. (2000), "Non-linear strains and stability of thin-walled bars", *J. Construct. Steel Res.*, **56**, 237-252.
- Barsoum, R. S. and Gallagher, R. H. (1970), "Finite element analysis of torsional and torsional-flexural stability problems", *Int. J. Numer. Methods Eng.*, **2**, 335-352.
- Bazant, Z. P. and El Nimeiri, M. (1973), "Large-deflection spatial buckling of thin walled beams and frames", *J. Eng. Mech. Div.*, ASCE, **99**, 1259-1281.
- Eurocode 3, (1992), *Design of steel structures, Part 1.1: General rules for buildings*. European Committee for standardization, Draft Document ENV 1993-1-1, Brussels.
- Hibbit, Karlsson and Sorensen Inc (2003), *Abaqus Standard User's Manual*, Version 6.4. Abaqus, Pawtucket, RI, USA.
- Laudiero, F. and Zaccaria, D. (1988), "A consistent approach to linear stability of thin-walled beams of open section", *Int. J. Mech. Sci.*, **30**, 503-515.
- Mohri, F., Azrar, L. and Potier-Ferry, M. (2001), "Flexural-torsional post-buckling analysis of thin-walled elements with open sections", *Thin-Walled Structures*, **39**, 907-938.
- Mohri, F., Azrar, L. and Potier-Ferry, M. (2002), "Lateral post-buckling analysis of thin-walled open section beams", *Thin-Walled Structures*, **40**, 1013-1036.
- Mohri, F., Brouki, A. and Roth, J. C. (2003), "Theoretical and numerical stability analyses of unrestrained mono-symmetric thin-walled beams", *J. Construct. Steel Res.*, **59**, 63-90.
- Pi, Y. L. and Bradford, M. A. (2001), "Effects of approximations in analyses of beams of open thin-walled cross-section, Part I: Flexural-torsional stability", *Int. J. Numer. Methods Eng.*, **51**, 757-772.
- Roberts, T. M. and Burt, C. A. (1985), "Instability of mono symmetric beams and cantilevers", *Int. J. Mech. Sci.*, **27**(5), 313-324.
- Ronagh, H. R., Bradford, M. A. and Attard, M. M. (2000), "Non-linear analysis of thin-walled members of variable cross-section, Part II: Application", *Comput. Struct.*, **77**, 301-313.
- Timoshenko, S. P. and Gere, J. M. (1961), *Theory of Elastic Stability*, 2nd edition, McGraw Hill, NY.
- Trahair, N. S. (1993), *Flexural-Torsional Buckling of Structures*, Chapman & Hall, London.
- Vacharajittiphan, P., Woolcock, S. T. and Trahair, N. S. (1974), "Effect of in-plane deformation on lateral buckling", *J. Struct. Mech.*, ASCE, **3**(11), 29-60.